Acta Pharmaceutica Sinica B 2025;15(8):4064−4077

Chinese Pharmaceutical Association
Institute of Materia Medica, Chinese Academy of Medical Sciences

Acta Pharmaceutica Sinica B

www.elsevier.com/locate/apsb
www.sciencedirect.com

ORIGINAL ARTICLE

Inhibition of WAC alleviates the chondrocyte proinflammatory secretory phenotype and cartilage degradation *via* H2BK120ub1 and H3K27me3 coregulation

Peitao Xu[a,†], Guiwen Ye[a,†], Xiaojun Xu[a,†], Zhidong Liu[a], Wenhui Yu[a], Guan Zheng[a], Zepeng Su[a], Jiajie Lin[a], Yunshu Che[a], Yipeng Zeng[a], Zhikun Li[a], Pei Feng[b], Qian Cao[b], Zhongyu Xie[a], Yanfeng Wu[b,*], Huiyong Shen[a,*], Jinteng Li[a,*]

[a]*Department of Orthopedics, the Eighth Affiliated Hospital of Sun Yat-sen University, Shenzhen 518003, China*
[b]*Center for Biotherapy, the Eighth Affiliated Hospital of Sun Yat-sen University, Shenzhen 518003, China*

Received 15 December 2024; received in revised form 19 February 2025; accepted 8 April 2025

KEY WORDS

Arthritis;
WAC;
Cartilage degradation;
Chondrocyte secretion;
Histone modification;
Doxercalciferol;
Molecular docking and dynamic simulation;
Inflammation

Abstract Several types of arthritis share the common feature that the generation of inflammatory mediators leads to joint cartilage degradation. However, the shared mechanism is largely unknown. H2BK120ub1 was reportedly involved in various inflammatory diseases but its role in the shared mechanism in inflammatory joint conditions remains elusive. The present study demonstrated that levels of cartilage degradation, H2BK120ub1, and its regulator WW domain-containing adapter protein with coiled-coil (WAC) were increased in cartilage in human rheumatoid arthritis (RA) and osteoarthritis (OA) patients as well as in experimental RA and OA mice. By regulating H2BK120ub1 and H3K27me3, WAC regulated the secretion of inflammatory and cartilage-degrading factors. WAC influenced the level of H3K27me3 by regulating nuclear entry of the H3K27 demethylase KDM6B, and acted as a key factor of the crosstalk between H2BK120ub1 and H3K27me3. The cartilage-specific knockout of WAC demonstrated the ability to alleviate cartilage degradation in collagen-induced arthritis (CIA) and collagenase-induced osteoarthritis (CIOA) mice. Through molecular docking and dynamic simulation, doxercalciferol was found to inhibit WAC and the development of cartilage degradation in the CIA

*Corresponding authors.
E-mail addresses: lijt57@mail.sysu.edu.cn (Jinteng Li), shenhuiy@mail.sysu.edu.cn (Huiyong Shen), wuyf@mail.sysu.edu.cn (Yanfeng Wu).
[†]These authors made equal contributions to this work.
Peer review under the responsibility of Chinese Pharmaceutical Association and Institute of Materia Medica, Chinese Academy of Medical Sciences.

https://doi.org/10.1016/j.apsb.2025.06.015

and CIOA models. Our study demonstrated that WAC is a key factor of cartilage degradation in arthritis, and targeting WAC by doxercalciferol could be a viable therapeutic strategy for treating cartilage destruction in several types of arthritis.

1. Introduction

Cartilage, a pivotal component in synovial joints, comprises chondrocytes as the exclusive cellular entities within the dense and intricately organized extracellular matrix (ECM)[1]. Chondrocytes embedded within the ECM instigate changes either directly or indirectly, inducing modifications in the ECM, thereby jeopardizing the integrity of cartilage[2]. This disruption can profoundly impact adjacent cells and tissues, ultimately resulting in joint dysfunction. Osteoarthritis (OA) and rheumatoid arthritis (RA) stand out as the 2 most prevalent disorders causing joint cartilage degradation, significantly affecting societal development, healthcare costs, and the daily lives of a considerable number of patients[3,4]. Despite distinct etiologies, both conditions exhibit common features, including the generation of inflammatory mediators such as TNF and IL-1β, culminating in joint cartilage degradation[5]. A notable similarity between RA and OA lies in the self-reinforcing and self-sustaining nature of cartilage degradation. Upon exposure to stimuli such as inflammatory mediators, chondrocytes secrete enzymes such as matrix metalloproteinases (MMP3 and MMP13) and chemokines (CCL2 and CCL3) with the capacity to degrade the cartilage matrix[6]. The degraded matrix, coupled with attracted inflammatory cells, further intensifies cartilage inflammation. Nevertheless, a comprehensive understanding of the shared mechanisms contributing to cartilage degradation in inflammatory joint conditions, such as RA and OA, is currently lacking. A more exhaustive investigation of these mechanisms holds substantial promise for advancing strategies to prevent and treat cartilage degradation in arthritis.

Histone modifications, including methylation, acetylation, and ubiquitination, play a pivotal role in the intricate regulation of gene expression through mechanisms such as chromosome folding modulation, nucleosome movement, and transcription factor recruitment. These modifications are integral to various physiological activities and processes underlying disease development[7,8]. The dysregulation of histone modifications has been widely implicated in the pathogenic mechanisms of arthritis[9-11]. Initially identified in 1980, H2BK120 monoubiquitination (H2BK120ub1) stands out as a hallmark of histone modifications, significantly influencing diverse nuclear processes, including gene transcription activation, higher-order chromatin organization, and the DNA damage response. Functionally, H2BK120ub1 inhibits the folding of nucleosome arrays and the oligomerization of fibers, thereby regulating chromatin accessibility and stability or recruiting specific effector proteins for chromatin-related activities[12]. The catalysis of H2BK120ub1 is orchestrated by the E3 ubiquitin ligase RNF20/40, which ubiquitinates H2B post-binding to the chromosome through WW domain-containing adapter protein with coiled-coil (WAC) association with RNA polymerase II (Pol II)[13]. In the context of cartilage development, H2BK120ub1 plays a crucial role, and its dysregulation contributes to the aggravation of various pathological processes by influencing inflammation levels[14-16]. Nevertheless, the specific involvement of abnormal levels of histone H2BK120ub1 in the initiation and progression of cartilage degradation and arthritis remains largely unexplored and necessitates further investigation.

A growing body of evidence suggests that H2BK120ub1 functions as a priming modification, orchestrating the regulation of additional histone modifications. The current focus revolves around modifications such as H3K4 methylation and H3K79 methylation, primarily associated with the activation of gene transcription[17,18]. The impact of H2BK120ub1 is predominantly observed in histone methylation, where it influences complexes such as methyltransferases[19,20]. However, scant research has explored the repercussions of H2BK120ub1 on other categories of histone methylations, particularly those associated with repressive histone methylation. Conducting additional studies is imperative to comprehensively unravel these intricate interactions and mechanisms.

In this study, we observed heightened expression of WAC and elevated levels of H2BK120ub1 in chondrocytes obtained from patients with both RA and OA. By regulating H2BK120ub1, WAC exhibited the capacity to modulate the secretion of inflammatory and cartilage-degrading factors in response to inflammatory stimuli. Moreover, through the control of the nuclear entry of the demethylase KDM6B, WAC influences the level of H3K27me3, subsequently impacting chondrocyte secretion. The cartilage-specific knockout of WAC alleviated cartilage degradation in collagen-induced arthritis (CIA) and collagenase-induced osteoarthritis (CIOA) mouse models. *Via* molecular docking and virtual screening strategies, doxercalciferol was found to reduce H2BK120ub1 levels by influencing the binding of WAC with Pol II and led to the alleviation of cartilage degradation in CIA and CIOA models. Our data highlighted that targeting WAC may emerge as a viable therapeutic strategy for treating cartilage destruction in several arthritis types.

2. Materials and methods

2.1. Human cartilage section biopsies

Human RA cartilage was obtained from patients undergoing total knee replacement surgery ($n = 3$; aged 51.7 ± 5.7 years; 1 male and 2 females). Human OA cartilage was collected from patients undergoing total knee replacement surgery ($n = 3$; aged 63.3 ± 3.5 years; 3 females). Normal control cartilage was obtained from a traffic accident victim who had no history of arthritis ($n = 3$; aged 34.7 ± 5.0 years; 2 males and 1 female). In this study, human cartilage was stained with safranin O/Fast green and examined by immunohistochemistry (IHC). Patient consent and the approval of the Ethics Committee of the Eighth Affiliated Hospital of Sun Yat-sen University (Shenzhen, China) were obtained before the human tissue samples were harvested (approval No. 23-048-01).

2.2. Animal models

Mice were used in the Laboratory Animal Center of Sun Yat-sen University and housed in cages under standard animal housing conditions with 12-h light and 12-h dark cycles. Mice in poor health were excluded from the study. All mouse experiments were approved by the animal ethics committee of Sun Yat-sen University (approval No. SYSU-IACUC-2022-000998).

2.2.1. $Wac^{fl/fl}$; *Col2*-Cre ERT^{+} conditional knockout (CKO) mice

C57BL/6 *Col2*-Cre ERT^{+} mice were purchased from Jackson Laboratory (Bar Harbor, ME, USA). C57BL/6 $Wac^{fl/fl}$ transgenic mice were purchased from Cyagen (Suzhou, China) to construct $Wac^{fl/fl}$; *Col2*-Cre ERT $^{+}$ CKO mice. The following PCR primers were used for genotyping $Wac^{fl/fl}$: 5′ arm primers, forward, TCCATCTCTTCCAACAAGTTGAGT, and 5′ arm primers reverse, CACATCTGACTTCAAAGTTCTTGC. In wild-type mice, only the 185-bp PCR product can be detected, and in homozygous $Wac^{fl/fl}$ mice, only the 248-bp PCR product can be detected. Both 185-bp and 248-bp PCR products were detected in heterozygous mice ($Wac^{fl/-}$). The *Col2*-Cre ERT $^{+}$ transgene was detected by PCR with primers detecting the Cre sequence in *Col2*-Cre ERT^{+} mice: *Col2*-Cre ERT^{+} forward, CACTGCGGGCT CTACTTCAT, and *Col2*-Cre ERT^{+} reverse, ACCAGCAGCACTT TTGGAAG. In *Col2*-Cre ERT^{+} mice, the 358-bp PCR product can be detected. To conditionally knock out *Wac* in *Col2*-Cre ERT^{+} mice, both the $Wac^{fl/fl}$ mice and *Col2*-Cre ERT^{+} mice were injected with tamoxifen (intraperitoneal injection, 75 mg/kg per day, 5 consecutive days).

2.2.2. Collagen-induced arthritis (CIA) mouse model

Mouse immunization was performed as described previously. To dissolve chicken CII (cCII; Sigma Chemical Co., St. Louis, MI, USA) in 0.1 mol/L acetic acid to 2.0 mg/mL by overnight rotation at 4 °C, Freund's complete adjuvant was mixed with an equal volume of *Mycobacterium tuberculosis* (2.5 mg/mL; Chondrex, Redmond, WA, USA) with 100 μL of emulsion administered intradermally on Day 0. On Day 21, the same injection was repeated. The hind limb ankle joints of the mice were collected on Day 42 after sacrifice.

2.2.3. Collagenase-induced osteoarthritis (CIOA) mouse model

Collagenase-induced osteoarthritis was induced in 12-week-old mice by injecting 1 U collagenase type VI (Sigma−Aldrich, Bornem, Belgium) into the right knee. The controls were the contralateral knees injected with PBS. In these models, mice were sacrificed, and the hind limb knee joints were collected after 7 days.

2.3. Statistical analysis

The data in this study were analyzed using SPSS 26.0. The results are expressed as the mean ± standard deviation (SD). Statistical analyses included Student's *t*-test, one-way analysis of variance followed by the Bonferroni correction, and the Pearson correlation test. A significance level of $P < 0.05$ was considered statistically significant.

Detailed experimental procedures and specific materials are described in the Supporting Information.

3. Results

3.1. Upregulation of H2BK120ub1 and WAC in cartilage tissues from RA and OA patients, CIA and CIOA mouse models

To investigate the role of H2BK120ub1 in cartilage degradation in inflammatory joint conditions, cartilage specimens were collected from RA patients, OA patients, and healthy controls. The results of safranin O/Fast green, immunohistochemistry staining, and Western blot revealed elevated H2BK120ub1 levels in RA and OA patient cartilage compared to healthy controls (Fig. 1A, Supporting Information Fig. S1A). Collagen-induced arthritis (CIA) and collagenase-induced osteoarthritis (CIOA) mouse models were used, because the CIA model is well characterized for studying RA[21] and the CIOA model is well characterized for studying early inflammation reaction in OA[22,23], and ankle joints of CIA and knee joints of CIOA were collected. Safranin O/Fast green, immunohistochemistry staining, and Western blot revealed cartilage degradation and elevated H2BK120ub1 levels in the CIA and CIOA model mice compared to negative controls (Fig. 1B, Fig. S1A).

Inflammatory joint conditions share the same feature: the generation of inflammatory cytokines stimulates chondrocytes to secrete MMPs and CCLs, which further intensifies cartilage degradation[24,25]. To evaluate the role of H2BK120ub1 in the cytokine-induced chondrocyte proinflammatory secretory phenotype, the levels of H2BK120ub1 in normal human chondrocytes and mouse chondrocytes after TNF or IL-1β stimulation were evaluated. The Western blot results showed that the levels of H2BK120ub1 in human chondrocytes and mouse chondrocytes were increased after cytokine stimulation (Fig. 1C, Fig. S1B).

There are multiple regulators of H2BK120ub1[26]. To further clarify the reasons for the upregulation of H2BK120ub1, we employed label-free quantitative proteomics to analyze the protein expression in normal human chondrocytes following TNF or IL-1β stimulation (Fig. 1D, Fig. S1C). In the Gene Ontology (GO) analyses for the biological process category, terms in both the TNF and IL-1β groups included Histone H2B ubiquitination (Fig. 1E). The results indicated that stimulation with TNF or IL-1β significantly upregulated the classical regulator of H2BK120ub1, the WW domain-containing adapter protein with coiled-coil (WAC) (Fig. 1F). Diminishing WAC in human mesenchymal stem cells suppresses the level of H2BK120ub1 has been described by previous reports[14,27]. Subsequently, we confirmed through Western blot analysis that TNF or IL-1β stimulation resulted in the upregulation of WAC in both human and mouse chondrocytes (Fig. S1D and S1E). The results of immunohistochemistry staining and Western blot revealed that the expression of WAC was upregulated in cartilage from RA, OA patients, and CIA, CIOA mouse models, compared to healthy controls (Fig. 1G and H, Fig. S1F). Taken together, these results indicated that the H2BK120ub1 level and WAC expression were increased in degraded cartilage in RA, OA patients, and CIA, CIOA mouse models.

3.2. Diminishing WAC alleviated the cytokine-induced chondrocyte proinflammatory secretory phenotype

To evaluate the biological and molecular consequences of H2BK120ub1 and WAC in the chondrocyte proinflammatory secretory phenotype, we used lentiviruses to diminish WAC in normal human chondrocytes (Supporting Information Fig. S2A and S2B). The results of qRT-PCR and Western blot demonstrated that knockdown of WAC decreased the expression of the

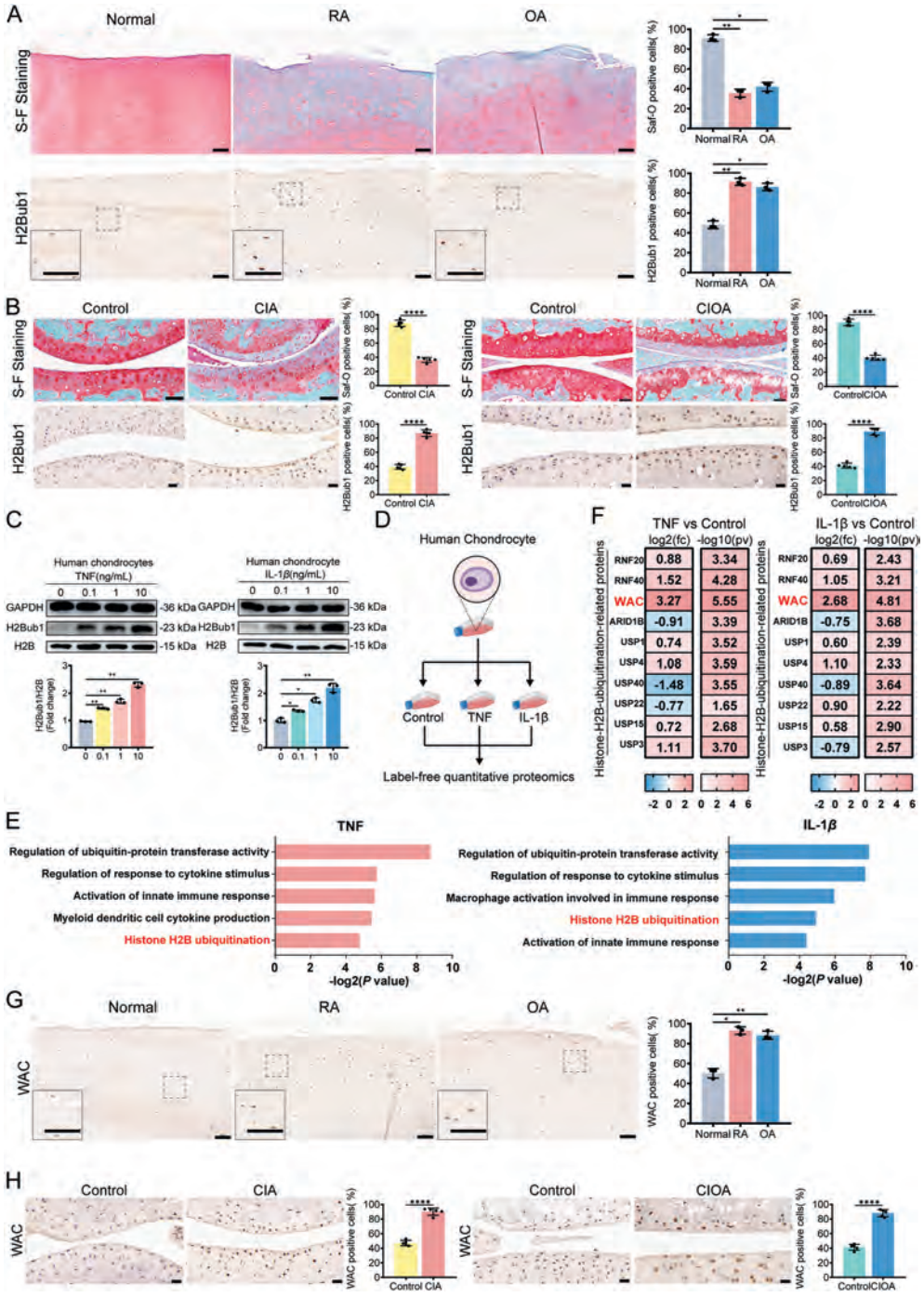

Figure 1 Upregulation of H2BK120ub1 and WW domain-containing adapter protein with coiled-coil (WAC) in cartilage tissues from rheumatoid arthritis (RA), osteoarthritis (OA) patients, and collagen-induced arthritis (CIA), collagenase-induced osteoarthritis (CIOA) mouse models. (A) Representative images of Safranin O/fast green (S−F) staining and immunohistochemistry (IHC) staining of H2BK120ub1 in normal, RA, and OA cartilage. Scale bars: 100 μm (top) and 50 μm (bottom and local enlarged). (B) Representative images of S−F staining and IHC staining of H2BK120ub1 in cartilage from control, CIA mice, and CIOA mice. Scale bars: 50 μm (top) and 20 μm (bottom). (C) Western blot analysis of H2BK120ub1 levels in TNF-treated (0, 0.1, 1, 10 ng/mL) or IL-1β-treated (0, 0.1, 1, 10 ng/mL) normal human chondrocytes. $n = 3$ per group. (D) Diagram showing the workflow of label-free quantitative proteomics. (E) GO analysis of the proteomics data between the differentially expressed genes in TNF *vs*. control. Bar graph showing the *P* values of the enriched terms. (F) $\log_2$(fold change) and $-\log_{10}(P$ value) of histone-H2B-monoubiquitination-related proteins expression between the TNF *vs*. control or IL-1β *vs*. control group as obtained from the proteomics data. TNF: 10 ng/mL, 24 h. IL-1β: 10 ng/mL, 24 h. (G) Representative images of immunohistochemistry (IHC) staining of WAC in normal, RA, and OA cartilage. Scale bars: 50 μm (original and local enlarged). (H) Representative images of IHC staining of WAC in cartilage from control and CIA mice and control and CIOA mice. Scale bars: 20 μm (bottom). All data are presented as the mean ± SD, $^*P < 0.05$, $^{**}P < 0.01$, $^{****}P < 0.0001$. H2Bub1 = H2BK120ub1.

proinflammatory factors MMP3, MMP13, CCL2 and CCL3 after TNF or IL-1β stimulation in three different cell types, including human chondrocytes, human chondrocyte C28/I2 cells and SW1353 cells (Fig. 2A and B, Supporting Information Fig. S3A and S3B).

Furthermore, we performed RNA-seq to study the impact of diminishing WAC in human chondrocytes after TNF stimulation. A heatmap showed distinct expression patterns before and after TNF stimulation and WAC knockdown (Fig. S2C). Protein−protein interaction network analysis was made based on protein WAC (Supporting Information Fig. S4). The gene set enrichment analysis (GSEA) of the RNA-seq data from the TNF/Sh-NC and TNF/Sh-WAC groups showed obvious enrichment of genes related to the inflammatory response, arthritis and cytokine-mediated signaling pathway (Fig. 2C). Furthermore, in GO analyses for the biological process category, the terms in which the differentially expressed genes in TNF/Sh-NC and TNF/Sh-WAC were enriched were closely related to cartilage degradation and chondrocyte pro-inflammatory secretory phenotype, including inflammatory response, chemokine-mediated signaling pathway, cellular response to tumor necrosis factor, extracellular matrix organization positive regulation of NIK/NF-κB signaling and extracellular matrix disassembly (Fig. 2D). Moreover, based on the RNA-seq results, we identified 44 intersecting genes from 508 upregulated genes in the TNF/Sh-NC group compared to the NC/Sh-NC group and 153 downregulated genes in the TNF/Sh-WAC group compared to the TNF/Sh-NC group (Supporting Information Fig. S5A). In GO analyses for the biological process category, the terms in which these genes were enriched included extracellular matrix disassembly, collagen catabolic process, cellular response to tumor necrosis factor, cellular response to interleukin-1, and immune response (Fig. S5B). The expression of proinflammatory secretory phenotype genes (*MMP3*, *MMP13*, *CCL2* and *CCL3*) from the NC/Sh-NC, TNF/Sh-NC and TNF/Sh-WAC human chondrocytes datasets confirmed that diminishing WAC decreased the expression of proinflammatory factors upregulated after TNF stimulation (Fig. 2E). The results mentioned above indicate that diminishing WAC alleviates the cytokine-induced proinflammatory secretory phenotype in chondrocytes.

3.3. Regulation of the recruitment of H2BK120ub1, H3K27me3, and p65 by WAC

A growing body of evidence suggests that H2BK120ub1 functions as a priming modification, orchestrating the regulation of additional histone modifications such as histone methylation, which is associated with gene transcription and silencing[19,28]. To investigate whether WAC directly affects histone methylation, we used lentiviruses to diminish and overexpress WAC in human chondrocytes (Supporting Information Fig. S6A and S6B). Western blot results revealed that WAC knockdown specifically increased trimethylation of H3 at lysine 27 (H3K27me3), while WAC overexpression reduced H3K27me3 (Fig. 3A). We next investigated the levels of histone trimethylation in NC/Sh-NC, TNF/Sh-NC and TNF/Sh-WAC human chondrocytes, and the results show that diminishing WAC increased the level of H3K27me3, which was reduced after TNF stimulation, while the increased H3K4me3 was not (Fig. 3B).

Various studies have demonstrated the important role of nuclear factor-κB (NF-κB) signaling in chondrocyte inflammatory responses and pro-inflammatory secretory phenotype. The results of GO analyses revealed that WAC could take part in regulation of NF-κB signaling (Fig. 2E). To further confirm the role of WAC in H2BK120ub1, H3K27me3 and p65 regulation, cleavage under targets and tagmentation sequence (CUT&Tag-seq) was used, and the heatmaps showing the general CUT&Tag-seq data signals revealed that loss of WAC reversed the significant increase in Pol II, H2BK120ub1 and p65 and reduction in H3K27me3 occupancy in the gene body in human chondrocytes after TNF stimulation (Fig. 3C). As expected, the occupancy of Pol II, H2BK120ub1 and p65 on *MMP3*, *MMP13*, *CCL2* and *CCL3*, which were examined by CUT&Tag-seq and CUT&Tag-qPCR, was reduced, and the occupancy of H3K27me3 was increased in the TNF/Sh-WAC groups (Fig. 3D, Fig. S6C−S6F). Furthermore, GO biological process analysis revealed that differentially expressed Pol II-, H2BK120ub1-, H3K27me3-and p65-occupied genes between the TNF/Sh-NC and TNF/Sh-WAC groups were enriched in terms related to cellular response to tumor necrosis factor, cellular response to interleukin-1, immune response and regulation of inflammatory response (Fig. 3E). Taken together, these observations suggest that WAC specifically regulates the monoubiquitination of H2B, trimethylation of H3K27, and the recruitment of NF-κB transcription factors.

3.4. WAC recruited KDM6B to regulate H3K27me3 and chondrocyte secretion

A massive amount of evidence suggests that H2BK120ub1 promotes the methylation of H3K4 and H3K79 by recruiting the histone methyltransferase complexes DOT1L and COMPASS[29,30]. However, the mechanism of the regulation of H3K27 methylation through H2B monoubiquitination remains poorly understood. To further investigate the mechanism by which WAC regulates H3K27me3, we used lentiviruses to diminish and overexpress WAC in human chondrocytes. The qRT-PCR and Western blot results demonstrated that WAC does not directly regulate the expression of the methyltransferase EZH2 or the demethylases KDM6A and KDM6B (Fig. 4A and B), which are reported to be regulators of H3K27me3[31-33]. Previous studies have shown that WAC serves as an adaptor to regulate H2BK120ub1 and mTOR activity[13,34]. The localization of histone methyltransferase and demethylases regulates the methylation of histones[35-37]. Therefore, we investigated the effect of WAC on the subcellular location of the methyltransferase EZH2 or the demethylases KDM6A and KDM6B. The Western blot results showed that diminishing WAC reduced nuclear KDM6B, while overexpressing WAC caused cytoplasmic accumulation of KDM6B (Fig. 4C). Furthermore, the results of immunofluorescence cell staining and coimmunoprecipitation further demonstrated that WAC regulates H3K27me3 by interacting with KDM6B and regulating its nuclear distribution (Fig. 4D and E).

To establish the role of KDM6B in the proinflammatory secretory phenotype of chondrocytes, we used lentiviruses to diminish KDM6B in chondrocytes (Supporting Information Fig. S7A). The qRT-PCR and Western blot results demonstrated that knockdown of KDM6B increased the level of H3K27me3 and decreased the expression of the proinflammatory factors MMP3, MMP13, CCL2, and CCL3 after TNF in human chondrocytes (Fig. 4F and G, Fig. S7B). GSK-J4 has been reported to be an inhibitor of the H3K27me3 demethylase KDM6B[38]. The qRT-PCR and Western blot results demonstrated that the inhibition of KDM6B by GSK-J4 increased the level of H3K27me3 and decreased the expression of the proinflammatory factors MMP3, MMP13, CCL2, and CCL3 after TNF in human chondrocytes (Fig. 4H and I, Fig. S7C). In summary, the results mentioned above indicate that diminishing WAC recruits KDM6B to regulate H3K27me3 and chondrocyte secretion.

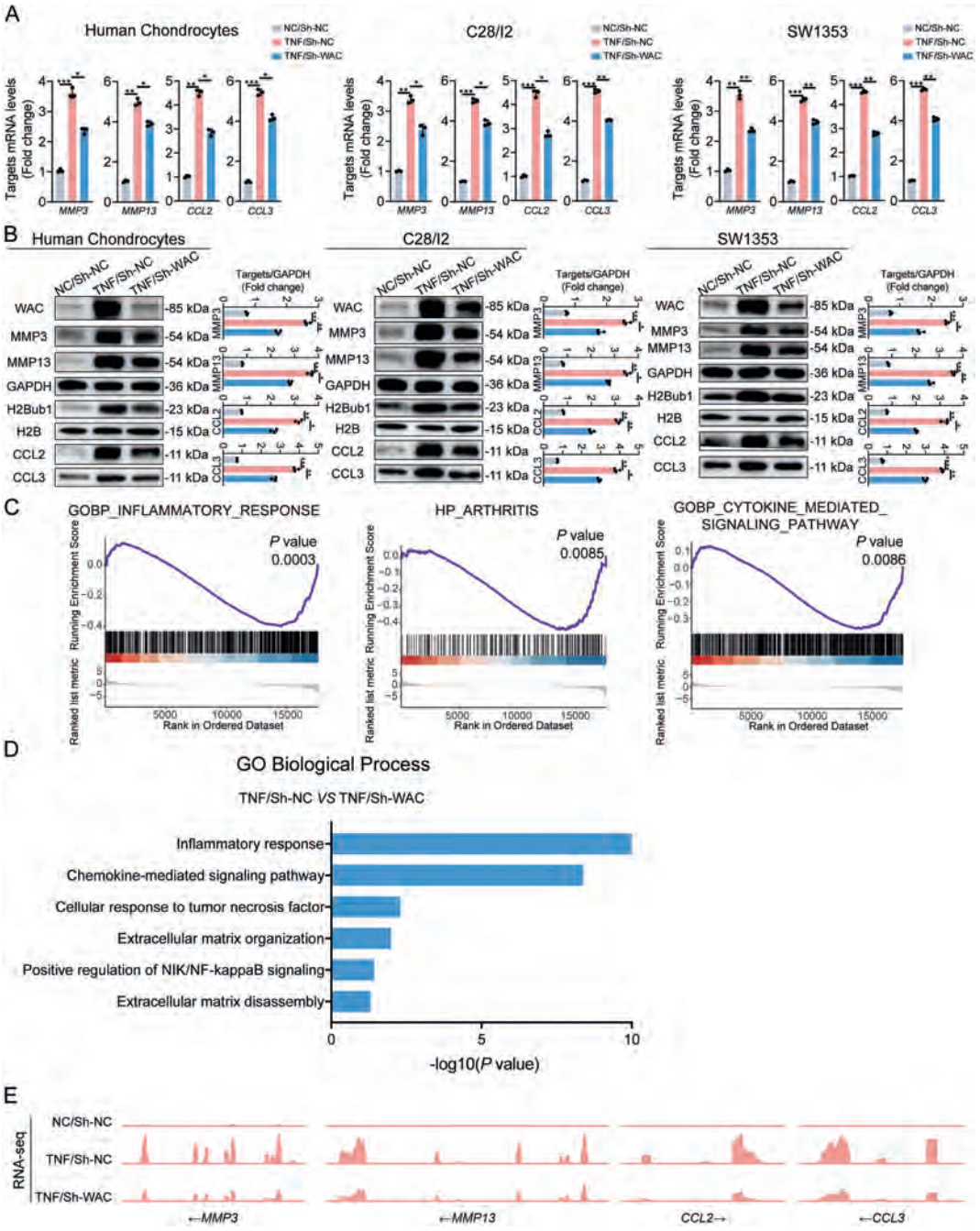

Figure 2 Diminishing WAC alleviated the TNF-induced chondrocyte proinflammatory secretory phenotype. (A) Quantitative real-time PCR analysis of *MMP3*, *MMP13*, *CCL2*, and *CCL3* expression in normal human chondrocytes, human chondrocyte C28/I2 cells, and SW1353 cells from the NC/Sh-NC, TNF/Sh-NC and TNF/Sh-WAC groups. GAPDH served as the internal control. (B) Western blot analysis of MMP3, MMP13, CCL2, and CCL3 expression and H2BK120ub1 levels in human chondrocytes, human chondrocyte C28/I2 cells, and SW1353 cells from the NC/Sh-NC, TNF/Sh-NC and TNF/Sh-WAC groups. GAPDH and H2B served as the internal controls. Bar graphs showing the relative levels. $n = 3$ per group. All data are presented as the mean ± SD, $^{*}P < 0.05$, $^{**}P < 0.01$, $^{***}P < 0.001$. (C) GSEA of the RNA-seq data between the human chondrocytes from the TNF/Sh-NC and TNF/Sh-WAC groups. (D) GO analysis of the RNA-seq data between the differentially expressed genes in TNF/Sh-NC and TNF/Sh-WAC. Bar graph showing the *P* values of the enriched terms. (E) RNA-seq analysis of MMP3, MMP13, CCL2, and CCL3 expression in human chondrocytes from the NC/Sh-NC, TNF/Sh-NC and TNF/Sh-WAC groups. TNF: 10 ng/mL, 24 h H2Bub1 = H2BK120ub1.

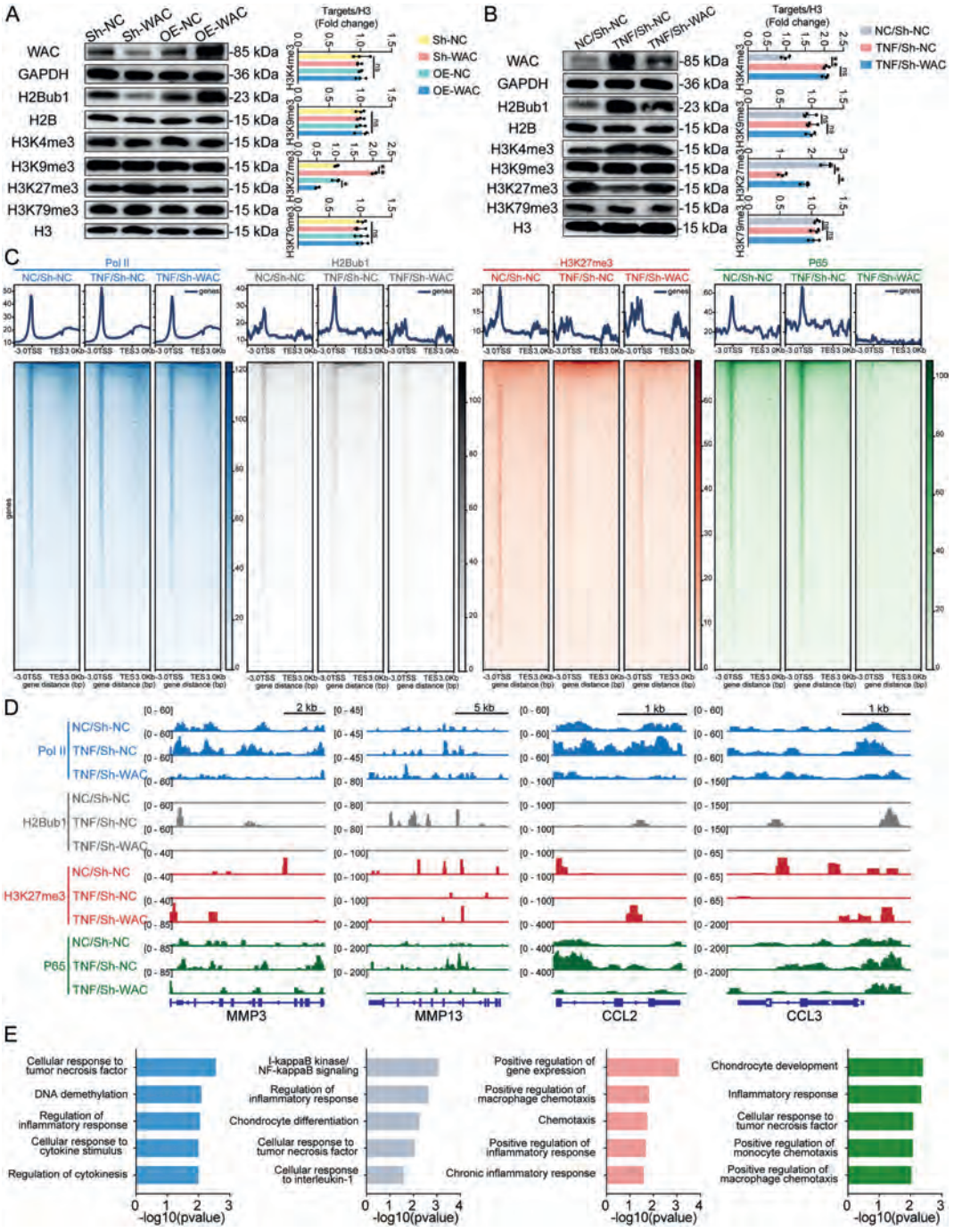

Figure 3 Regulation of the recruitment of H2BK120ub1, H3K27me3, and p65 by WAC. (A) Western blot analysis of H3K4me3, H3K9me3, H3K27me3, H3K79me3, and H2BK120ub1 levels in human chondrocytes from the Sh-NC, Sh-WAC, OE-NC and OE-WAC groups. H2B and H3 served as the internal controls. Bar graphs showing the relative levels. (B) Western blot analysis of H3K4me3, H3K9me3, H3K27me3, H3K79me3 and H2BK120ub1 levels in human chondrocytes from the NC/Sh-NC, TNF/Sh-NC and TNF/Sh-WAC groups. H2B and H3 served as the internal controls. Bar graphs showing the relative levels. (C) CUT&Tag-seq average binding profiles and heatmaps depicting the occupancy of Pol II, H2BK120ub1, H3K27me3, and p65 in human chondrocytes from the NC/Sh-NC, TNF/Sh-NC and TNF/Sh-WAC groups. (D) Signal traces of CUT&Tag-seq data showing Pol II, H2BK120ub1, H3K27me3, and p65 occupancy on MMP3, MMP13, CCL2, and CCL3 expression in human chondrocytes from the NC/Sh-NC, TNF/Sh-NC and TNF/Sh-WAC groups. (E) GO biological process analyses of the CUT&Tag-seq data comparing the human chondrocytes from the TNF/Sh-NC and TNF/Sh-WAC groups. Bar graph showing the P values of the enriched terms. The data are presented as the mean ± SD, $n = 3$, $^{*}P < 0.05$, $^{**}P < 0.01$; ns, no significance. TNF: 10 ng/mL, 24 h H2Bub1 = H2BK120ub1.

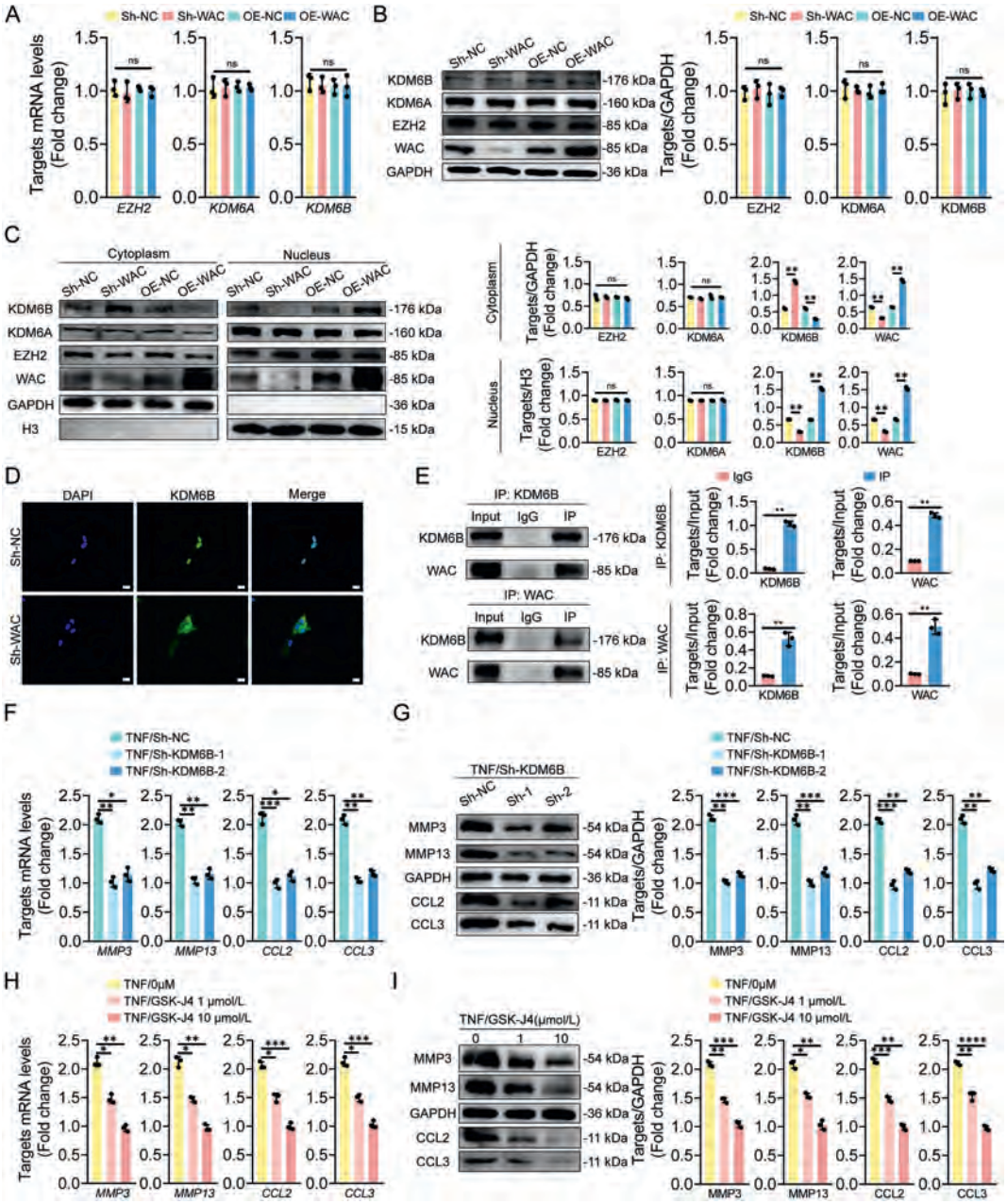

Figure 4 WAC recruited KDM6B to regulate H3K27me3 and chondrocyte secretion. (A) Quantitative real-time PCR analysis of EZH2, KDM6A, and KDM6B levels in human chondrocytes from the Sh-NC, Sh-WAC, OE-NC, and OE-WAC groups. (B) Western blot analysis of EZH2, KDM6A, and KDM6B levels in human chondrocytes from the Sh-NC, Sh-WAC, OE-NC, and OE-WAC groups. Bar graphs showing the relative levels. (C) Western blot analysis of EZH2, KDM6A, and KDM6B levels in the cytoplasm and nucleus in human chondrocytes from the Sh-NC, Sh-WAC, OE-NC, and OE-WAC groups. (D) Immunofluorescence staining (scale bar = 20 μm) showed the KDM6B nuclear distribution in the human chondrocytes from the Sh-NC and Sh-WAC groups. (E) The interaction between WAC and KDM6B was detected. (F, G) qRT-PCR and Western blot analysis of MMP3, MMP13, CCL2 and CCL3 expression in human chondrocytes from the TNF/Sh-NC, TNF/Sh-KDM6B-1, and TNF/Sh-KDM6B-2 groups. (H, I) qRT-PCR and Western blot analysis of MMP3, MMP13, CCL2, and CCL3 expression in human chondrocytes from the TNF/NC, TNF/GSK-J4 1 μmol/L and TNF/GSK-J4 10 μmol/L groups. Bar graphs showing the relative levels. All data are presented as the mean ± SD, $*P < 0.05$, $**P < 0.01$, $***P < 0.001$, $****P < 0.0001$; ns, no significance. TNF: 10 ng/mL, 24 h.

3.5. WAC deficiency alleviated chondrocyte secretion and cartilage degradation in the CIA and CIOA mouse models

To confirm the role of WAC and H2BK120ub1 in cartilage destruction in RA and OA, *Wac*$^{fl/fl}$ mice were constructed using the CRISPR−Cas9 technique. These mice were crossed with Col2-Cre ERT $^{+}$ mice to generate *Wac*$^{fl/fl}$; *Col2*-Cre ERT^{+} mice with tamoxifen-treated conditional knockout (CKO) of *Wac* in chondrocytes, collagen-induced arthritis (CIA) and collagenase-induced osteoarthritis (CIOA) mouse models were generated, and CIA ankle joints and CIOA knee joints were collected (Fig. 5A). Genotyping (Supporting Information Fig. S8A and

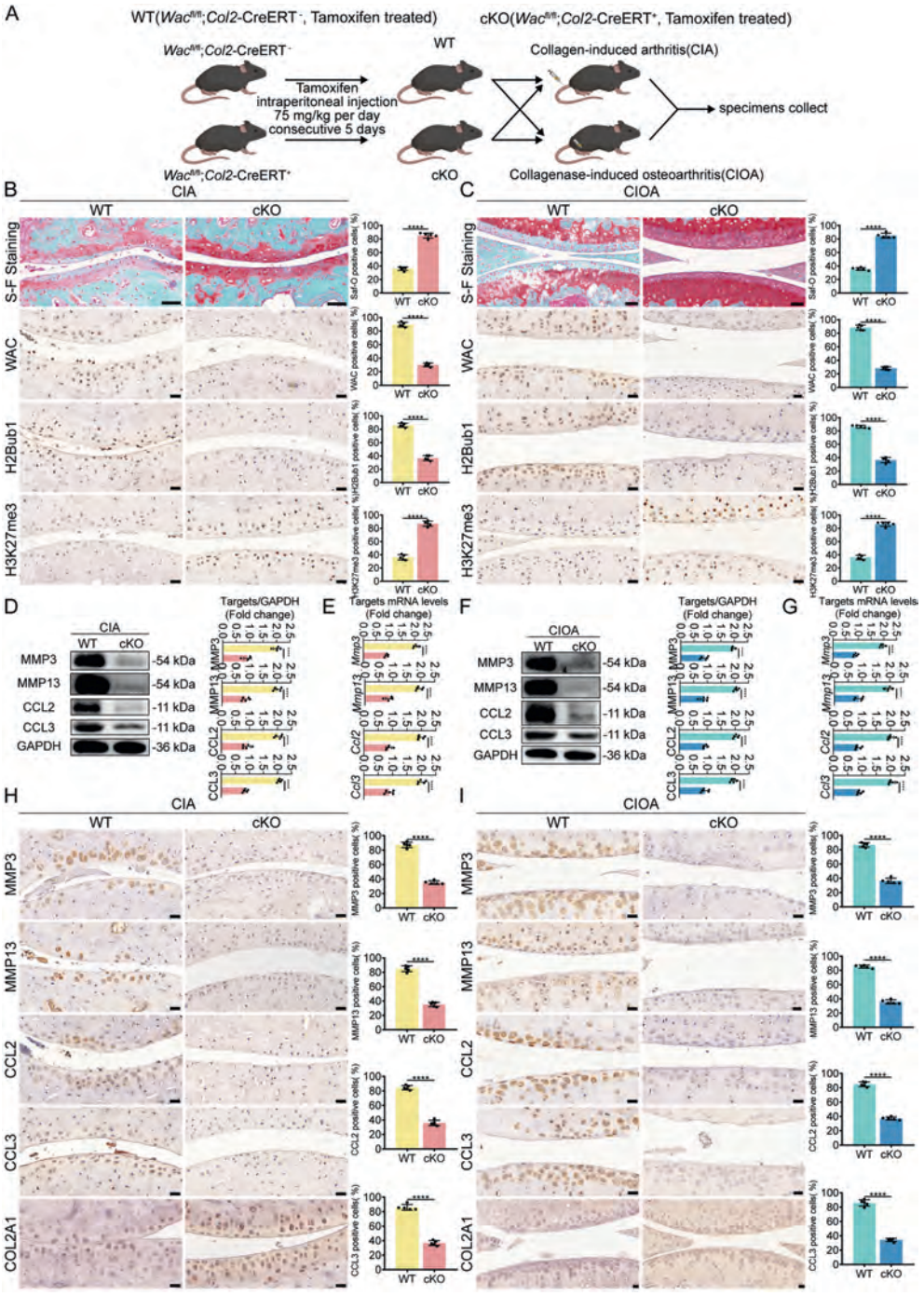

Figure 5 WAC deficiency alleviated chondrocyte secretion and cartilage degradation in the CIA and CIOA mouse models. (A) Diagram showing the workflow of CIA and CIOA mouse model induction in tamoxifen-treated $Wac^{fl/fl}$; *Col2*-Cre ERT^{+} mice (cKO) and $Wac^{fl/fl}$ mice (WT). (B, C) Representative images of S−F staining and IHC staining of WAC, H2BK120ub1, and H3K27me3 in cartilage from WT, CIA mice, and CIOA mice. Scale bars: 50 μm (top) and 20 μm (middle and bottom). Quantitative analysis of Safranin O and WAC, H2BK120ub1, and H3K27me3-positive chondrocytes as a proportion of the total chondrocytes. (D, E) Western blot and quantitative real-time PCR analysis of MMP3, MMP13, CCL2, and CCL3 in WT and cKO CIA cartilage. (F, G) Western blot and qRT-PCR analysis of MMP3, MMP13, CCL2, and CCL3 in WT and cKO CIOA cartilage. (H, I) Representative images of IHC staining of MMP3, MMP13, CCL2, CCL3, and COL2A1 in cartilage from WT and cKO CIA mice and CIOA mice. Scale bars: 20 μm. Quantitative analysis of MMP3-, MMP13-, CCL2-and CCL3-positive chondrocytes as a proportion of the total chondrocytes. All data are presented as the mean ± SD, $n = 5$ per group, $^{****}P < 0.0001$. H2Bub1 = H2BK120ub1.

S8B) verified the specific knockout of *Wac* in chondrocytes. Upon knocking out *Wac* in chondrocytes, $Wac^{fl/fl}$; *Col2*-Cre ERT $^{+}$ mice presented with less cartilage degradation than $Wac^{fl/fl}$ control mice in the CIA and CIOA mouse models, as shown by the results of Safranin O/Fast green staining of the cartilage (Fig. 5B and C). The immunohistochemistry staining results showed decreased levels of WAC and H2BK120ub1 and increased levels of H3K27me3 in cartilages in $Wac^{fl/fl}$; *Col2*-Cre ERT $^{+}$ mice compared to $Wac^{fl/fl}$ control mice (Fig. 5B and C). Furthermore, the chondrocytes extracted from $Wac^{fl/fl}$; *Col2*-Cre ERT^{+} mice showed decreased levels of MMP3, MMP13, CCL2, CCL3, WAC and H2BK120ub1 and increased levels of H3K27me3, as shown by the qRT−PCR and Western blot results (Fig. 5D−G, Fig. S9A−S9D). The immunohistochemistry staining results demonstrated that, in $Wac^{fl/fl}$; Col2-Cre ERT + mice, the expression of MMP3, MMP13, CCL2, and CCL3 in cartilage was downregulated compared to $Wac^{fl/fl}$ control mice, while the marker for extracellular matrix synthesis, type II collagen (COL2A1), was increased (Fig. 5H and I). Together, these results indicated that WAC deficiency alleviates chondrocyte secretion and cartilage degradation in the CIA and CIOA mouse models.

3.6. The WAC inhibitor Dox alleviated chondrocyte secretion and cartilage degradation in vitro and in vivo

To identify an available drug targeting the WW domain of WAC to decrease H2BK120ub1 to alleviate chondrocyte secretion and cartilage degradation, molecular docking and virtual screening strategies were used. Among the top 10 drugs screened from 1615 FDA-approved drugs, doxercalciferol showed the best effect in decreasing the expression of the proinflammatory secretory phenotype in human chondrocytes, as shown by the qRT-PCR results (Fig. 6A and B, Supporting Information Fig. S10). The results of the potential energy plot and root-mean-square deviation (RMSD) supported the potential interaction between WAC and doxercalciferol (Fig. 6C and D). The Western blot analysis showed that the level of H2BK120ub1 and the expression of MMP3, MMP13, CCL2 and CCL3 were downregulated by doxercalciferol at concentrations of 1, 2.5, and 5 μmol/L in a dose-dependent manner (Fig. 6E). Furthermore, the coimmunoprecipitation results demonstrated that doxercalciferol treatment disturbed the combination of WAC and Pol II, which led to a decrease in H2BK120ub1 (Fig. 6F).

We then evaluated the effect of doxercalciferol in the CIA and CIOA mouse models, and the mice were treated with doxercalciferol (100 ng/kg, i.p., thrice per week) after the mouse models were induced. The doxercalciferol and saline treatment groups in negative control mice were included to exclude any independent effects outside of the CIA or CIOA models. Safranin O/Fast green staining and immunohistochemistry analysis of the cartilage showed no significant differences in cartilage degradation or chondrocyte secretion between the doxercalciferol and saline treatment groups in these negative controls (Supporting Information Fig. S11A). As shown by the results of the Safranin O/Fast green and immunohistochemistry staining of the cartilage, cartilage degradation and H2BK120ub1 levels were decreased in the doxercalciferol-treated group in the CIA and CIOA mouse models (Fig. 6G and H). As shown by immunohistochemistry staining, the expression of MMP3, MMP13, CCL2 and CCL3 in cartilage in the doxercalciferol-treated group was downregulated and COL2A1 was increased compared to that in the saline-treated group (Fig. 6I and J). Furthermore, chondrocytes extracted from the doxercalciferol-treated group showed lower levels of MMP3, MMP13, CCL2, CCL3, and H2BK120ub1 than those from the saline-treated group, as shown by the qRT-PCR and Western blot results (Fig. S11B and S11C). Together, these results indicated that the WAC inhibitor doxercalciferol decreased H2BK120ub1 levels and alleviated chondrocyte secretion and cartilage degradation *in vitro* and *in vivo*.

4. Discussion

Cartilage, consisting of chondrocytes, constitutes a vital element within joints, showcasing remarkable durability under healthy conditions. However, its inherent regenerative capacity is limited, and once subjected to damage, cartilage experiences gradual degradation, culminating in impaired joint function. Rheumatoid arthritis (RA) and osteoarthritis (OA) emerge as 2 prevalent chronic inflammatory diseases responsible for cartilage degeneration[3,4]. Despite cartilage degradation being a shared characteristic of joint conditions such as RA and OA, directly comparing the processes of these 2 diseases proves to be a challenging yet essential endeavor. RA is acknowledged as a systemic inflammatory disease with a significant impact on joints, and its etiology remains incompletely understood. The pathogenesis primarily involves systemic and local immune reactions that activate synovial cells, including fibroblasts, leading to the assault on cartilage and subsequent damage[39-41]. However, mounting research indicates altered metabolic conditions in the chondrocytes of RA. In contrast, OA is a degenerative joint disease where damage to joint cartilage is believed to stem from factors such as mechanical stress and inflammatory agents, which stimulate the intrinsic activities of chondrocytes[42]. Despite differing etiologies, inflammatory factors such as TNF and IL-1β are recognized to play crucial roles in the occurrence and development of both RA and OA[43,44].

A common pathological manifestation in RA and OA involves the abnormal secretion of matrix-degrading enzymes, including those of the MMP family, by chondrocytes, leading to cartilage degradation[6]. Despite extensive experimental evidence highlighting the pivotal role of these enzymes in RA and OA, nearly all clinical trials involving MMP inhibitors, including MMP2, MMP3, MMP9, and MMP13, among others, have encountered failure[45]. Furthermore, concerns regarding musculoskeletal toxicity associated with MMP inhibitors remain unresolved[46]. In recent years, there has been a growing focus on the production of cytokines and chemokines by stimulated chondrocytes, further fueling the development of arthritis[47,48]. Therefore, unraveling the specific mechanisms underlying the production of factors such as MMPs and CCLs by chondrocytes in response to stimuli is crucial. It holds promise as a key target for the prevention and treatment of cartilage destruction progress in arthritis.

A plethora of research underscores the role of histone modifications as signals for either transcriptional activation or inhibition. Specifically, ubiquitination of the K120 residue on H2B and methylation of K4/36/79 residues on H3 are associated with transcriptional activation, while ubiquitination of K119 on H2A and methylation of K9/27 on H3 are correlated with transcriptional repression[33]. In recent years, growing attention has been devoted to unraveling the significance of histone modifications in arthritis and cartilage growth, as exemplified by some notable studies. However, the role of H2BK120ub1 in cartilage degradation in arthritis remains unexplored.

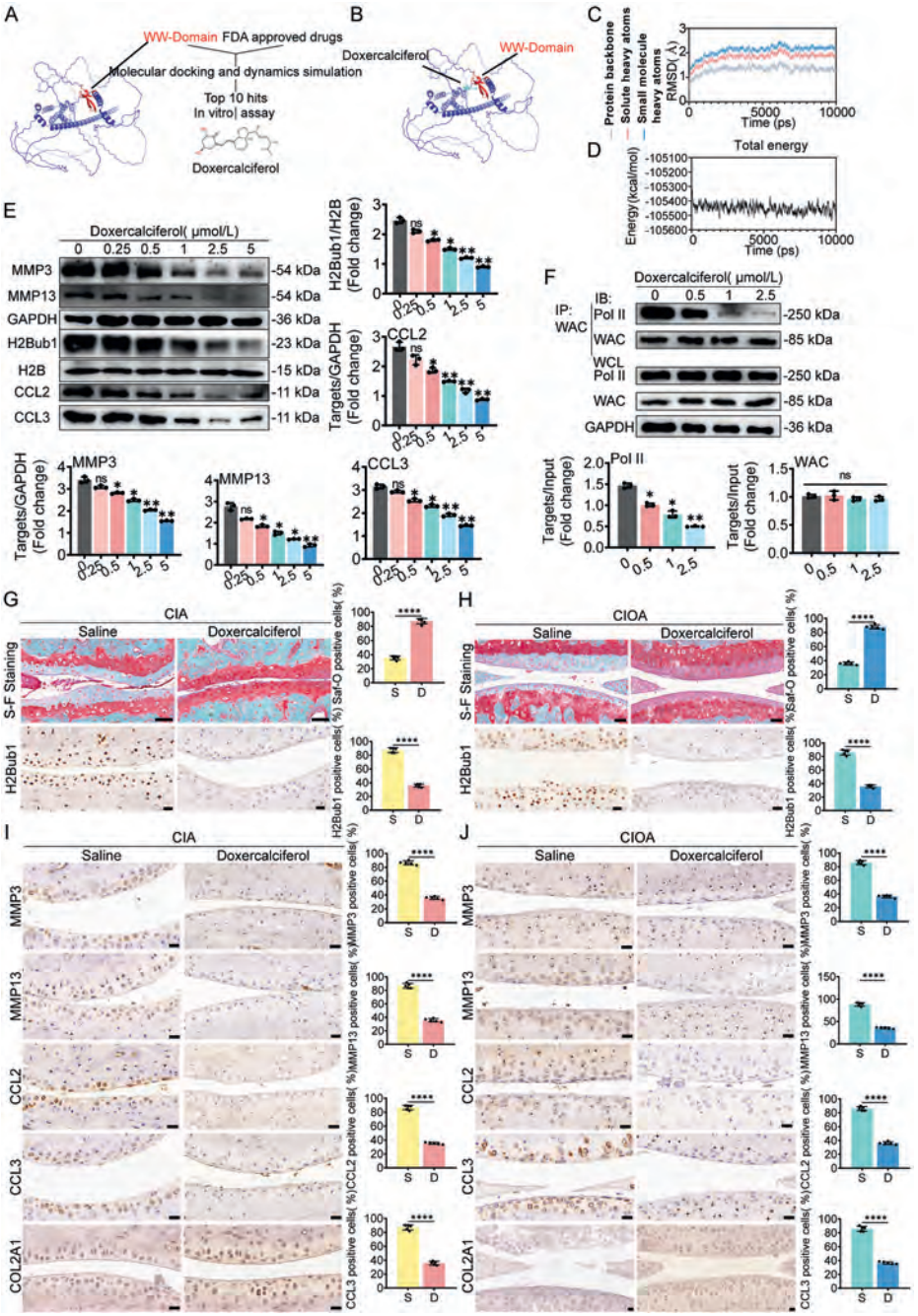

Figure 6 WAC inhibitor doxercalciferol alleviated chondrocyte secretion and cartilage degradation *in vitro* and *in vivo*. (A) Workflow of the molecular docking and virtual screening strategy. (B) Molecular docking demonstrated that doxercalciferol physically bound to the WW domain of WAC. (C, D) The results of the potential energy plot and root-mean-square deviation (RMSD) detected the interaction between WAC and doxercalciferol. (E) Western blot of MMP3, MMP13, CCL2, CCL3, and H2BK120ub1 in doxercalciferol-treated groups with TNF stimulation. (F) The interaction between WAC and Pol II in the doxercalciferol-treated groups was detected. (G, H) Representative images of S−F staining and IHC staining of H2BK120ub1 in cartilage from the saline and doxercalciferol groups in CIA mice and CIOA mice. Scale bars: 50 μm (top) and 20 μm (bottom). S = Saline, D = Doxercalciferol. (I, J) Representative images of IHC staining of MMP3, MMP13, CCL2, CCL3, and COL2A1 in cartilage from saline and doxercalciferol groups in CIA mice and CIOA mice. Scale bars: 20 μm. All data are presented as the mean ± SD, $n = 5$ per group, $^{*}P < 0.05$, $^{**}P < 0.01$, $^{****}P < 0.0001$; ns, no significance. H2Bub1 = H2BK120ub1.

In our study, we observed an elevation in the levels of H2BK120ub1 and its regulatory protein, WAC, in the cartilage of patients with RA and OA. Diminishing the expression of WAC resulted in chondrocytes expressing lower levels of MMP3, MMP13, CCL2, CCL3, and related factors, thereby mitigating the severity of cartilage degradation in arthritis. While research on H2BK120ub1 in inflammation is abundant, the majority of it is centered around ubiquitin ligases and deubiquitinating enzymes. Notably, WAC itself does not function as a ubiquitin ligase or a deubiquitinating enzyme; rather, it serves as a connecting protein

in the RNF20/40 ubiquitin ligase complex, facilitating the interaction between RNF20/40 and Pol II. WAC, being an evolutionarily conserved protein, plays a crucial role, particularly through its essential domains, namely, the WW domain and the coiled-coil region. Our research findings validate the role of WAC in the occurrence and progression of cartilage degradation in arthritis, underscoring its potential value as a therapeutic target.

Beyond its acknowledged role in chromatin structure modulation, H2BK120ub1 is considered a prerequisite for various activating histone methylations. Over the past few decades, research has elucidated that H2BK120ub1, by recruiting the histone methyltransferase complexes DOT1L and COMPASS, regulates the methylation of H3K4 and H3K79. Additionally, it influences histone demethylases in controlling H3K4 methylation. However, further investigation is needed to fully understand the impact of H2BK120ub1 on other histone methylation types. Our study revealed that WAC knockdown led to an elevation in H3K27me3 levels. Subsequent experiments indicated that WAC does not directly regulate the expression of the methyltransferase EZH2 or the demethylases KDM6A and KDM6B. The nuclear−cytoplasmic distribution experiments demonstrated that WAC can modulate the nuclear−cytoplasmic distribution of KDM6B but does not influence the other 2 proteins. These results unveil crosstalk between H2BK120ub1 and H3K27me3 through WAC/KDM6B in the regulation of cartilage degradation.

H3K27me3 is considered a signal for transcriptional repression, with the methyltransferase EZH2 and demethylases KDM6A and KDM6B playing roles in its regulation[31,32]. Although H3K27me3 is associated with heterochromatin, the mechanisms underlying its gene silencing remain incompletely understood. H3K27me3 is implicated in growth and development, cancer initiation and metastasis, and inflammation regulation, with reported connections to bone-related diseases[49]. Previous studies have indicated that knockout of KDM6B affects cartilage development and accelerates osteoarthritis progression in a destabilization of the medial meniscus (DMM) mouse model[50]. However, more recent research suggests that inhibiting KDM6B protects cartilage, slows joint deterioration, and exhibits anti-inflammatory effects[51,52]. Our experimental findings demonstrate that inhibiting KDM6B reduces the secretion of factors such as MMP and CCL by chondrocytes, thereby decreasing cartilage degradation. WAC, through its modulation of KDM6B's nuclear−cytoplasmic distribution, influences the enrichment levels of H3K27me3 on MMP3, CCLs, and other factors, affecting their expression.

Molecular docking, widely acknowledged as a prominent and successful method in structure-based drug design, refers to the reciprocal recognition process between 2 or more molecules through geometric and energy matching[53]. In recent years, molecular docking has become a pivotal approach for virtual screening of conventional drugs, aiding in early-stage drug discovery and identification of novel targets[54]. Through molecular docking and virtual screening, we identified doxercalciferol from the FDA-approved drug library as a potential therapeutic agent for cartilage injury. Doxercalciferol, a vitamin D2 analog, exerts its effects by binding to the vitamin D receptor. Vitamin D and its analogs regulate intestinal calcium absorption, renal tubular reabsorption of calcium in conjunction with parathyroid hormone, and calcium conversion in bones[55]. Clinically, doxercalciferol is mainly used for osteoporosis, chronic kidney disease, and secondary hyperparathyroidism[56,57]. Vitamin D has been reported to improve symptoms of joint-related disorders such as RA and OA, enhancing overall quality of life[58]. Several previous studies have already indicated the potent anti-inflammatory function of doxercalciferol, although the concrete mechanism is unclear. To our knowledge, we are the first to reveal that doxercalciferol could block the connection between WAC and POL II to inhibit H2BK120ub1 levels, which further suppresses proinflammatory factor release. We believe this mechanism is prone to be universal. Blocking the connection between WAC and POL II to inhibit H2BK120ub1 levels *via* doxercalciferol is worth further study in treating other inflammatory disorders.

However, this study has certain limitations. First, while an increase in WAC expression was observed in the cartilage of RA and OA patients, there was no significant alteration at the mRNA level. This implies that the overexpression of WAC may be attributed to posttranslational modifications. Moreover, despite regulating the H2BK120ub1 level, WAC also promotes the interaction between TTT and Pontin/Reptin, thereby promoting mTORC1 activity by facilitating mTORC1 dimerization and the mTORC1-Rag interaction[34]. Thus, overexpression of WAC leads to abnormal mTOR activation and autophagy inhibition. Several studies have already confirmed that autophagy defects could lead to several arthritis pathologies, including OA and RA[59,60]. Targeting WAC for autophagy defect rectification is an intriguing and promising strategy for treating cartilage destruction in arthritis. However, no further investigations were conducted concerning these mentioned aspects in this study. These gaps will be our future research focus.

5. Conclusions

In summary, our study identifies WAC and H2BK120ub1 as crucial factors in RA and OA-related cartilage injury. WAC modulates inflammatory factor secretion in chondrocytes, influencing H2BK120ub1 and H3K27me3. Both WAC knockout and doxercalciferol administration alleviate cartilage degradation in CIA and CIOA models. These results underscore WAC as a promising target for treating arthritis-associated cartilage destruction.

Acknowledgments

This study was supported by the Guangdong Provincial Clinical Research Center for Orthopedic Diseases (2023B110001, China), the National Natural Science Foundation of China (82172349, 82002267, 82102529), the Project Supported by Guangdong Natural Science Foundation (2023A1515010531, China), the Shenzhen Science and Technology Program (JCYJ20210324115007019, RCBS20221008093103013, China), and Futian Healthcare Research Project (FTWS2022020, FTWS2023058, China).

Author contributions

Peitao Xu: Writing − review & editing, Writing − original draft, Methodology, Conceptualization. Guiwen Ye: Writing − original draft, Methodology. Xiaojun Xu: Methodology. Zhidong Liu: Methodology. Wenhui Yu: Conceptualization. Guan Zheng: Methodology, Funding acquisition. Zepeng Su: Investigation. Jiajie Lin: Investigation. Yunshu Che: Investigation. Yipeng Zeng: Investigation. Zhikun Li: Investigation. Pei Feng: Investigation. Qian Cao: Investigation. Zhongyu Xie: Writing − review & editing, Supervision. Yanfeng Wu: Writing − review & editing,

Supervision, Funding acquisition. Huiyong Shen: Writing − review & editing, Supervision, Funding acquisition. Jinteng Li: Writing − review & editing, Writing − original draft, Methodology, Investigation, Funding acquisition, Conceptualization.

Conflicts of interest

The authors declare no competing interests.

Appendix A. Supporting information

Supporting information to this article can be found online at https://doi.org/10.1016/j.apsb.2025.06.015.

References

1. Aicher WK, Rolauffs B. The spatial organisation of joint surface chondrocytes: review of its potential roles in tissue functioning, disease and early, preclinical diagnosis of osteoarthritis. *Ann Rheum Dis* 2014;**73**:645−53.
2. Muthu S, Korpershoek JV, Novais EJ, Tawy GF, Hollander AP, Martin I. Failure of cartilage regeneration: emerging hypotheses and related therapeutic strategies. *Nat Rev Rheumatol* 2023;**19**:403−16.
3. Hunter DJ, Bierma-Zeinstra S. Osteoarthritis. *Lancet* 2019;**393**: 1745−59.
4. Smolen JS, Aletaha D, McInnes IB. Rheumatoid arthritis. *Lancet* 2016;**388**:2023−38.
5. Pap T, Korb-Pap A. Cartilage damage in osteoarthritis and rheumatoid arthritis—two unequal siblings. *Nat Rev Rheumatol* 2015;**11**:606−15.
6. Wang T, He C. Pro-inflammatory cytokines: the link between obesity and osteoarthritis. *Cytokine Growth Factor Rev* 2018;**44**:38−50.
7. Wang X, Xu J, Sun Y, Cao S, Zeng H, Jin N, et al. Hedgehog pathway orchestrates the interplay of histone modifications and tailors combination epigenetic therapies in breast cancer. *Acta Pharm Sin B* 2023; **13**:2601−12.
8. Liu R, Li Y, Zheng Q, Ding M, Zhou H, Li X. Epigenetic modification in liver fibrosis: promising therapeutic direction with significant challenges ahead. *Acta Pharm Sin B* 2024;**14**:1009−29.
9. Monteagudo S, Cornelis FMF, Aznar-Lopez C, Yibmantasiri P, Guns LA, Carmeliet P, et al. DOT1L safeguards cartilage homeostasis and protects against osteoarthritis. *Nat Commun* 2017;**8**:15889.
10. Yin Y, Yang X, Wu S, Ding X, Zhu H, Long X, et al. Jmjd1c demethylates STAT3 to restrain plasma cell differentiation and rheumatoid arthritis. *Nat Immunol* 2022;**23**:1342−54.
11. Dong Y, Chen Y, Ma G, Cao H. The role of E3 ubiquitin ligases in bone homeostasis and related diseases. *Acta Pharm Sin B* 2023;**13**: 3963−87.
12. Wu Z, Liu J, Zhang Q Di, Lv DK, Wu NF, Zhou JQ. Rad6-Bre1-mediated H2B ubiquitination regulates telomere replication by promoting telomere-end resection. *Nucleic Acids Res* 2017;**45**:3308−22.
13. Zhang F, Yu X. WAC, a functional partner of RNF20/40, regulates histone H2B ubiquitination and gene transcription. *Mol Cell* 2011;**41**: 384−97.
14. Karpiuk O, Najafova Z, Kramer F, Hennion M, Galonska C, König A, et al. The histone H2B monoubiquitination regulatory pathway is required for differentiation of multipotent stem cells. *Mol Cell* 2012; **46**:705−13.
15. Zhao Z, Su Z, Liang P, Liu D, Yang S, Wu Y, et al. USP38 couples histone ubiquitination and methylation *via* KDM5B to resolve inflammation. *Adv Sci* 2020;**7**:1−14.
16. Tarcic O, Pateras IS, Cooks T, Shema E, Kanterman J, Ashkenazi H, et al. RNF20 links histone H2B ubiquitylation with inflammation and inflammation-associated cancer. *Cell Rep* 2016;**14**:1462−76.
17. Wang E, Kawaoka S, Yu M, Shi J, Ni T, Yang W, et al. Histone H2B ubiquitin ligase RNF20 is required for MLL-rearranged leukemia. *Proc Natl Acad Sci U S A* 2013;**110**:3901−6.
18. Kim J, Guermah M, McGinty RK, Lee JS, Tang Z, Milne TA, et al. RAD6-mediated transcription-coupled H2B ubiquitylation directly stimulates H3K4 methylation in human cells. *Cell* 2009;**137**:459−71.
19. Jeon J, McGinty RK, Muir TW, Kim JA, Kim J. Crosstalk among Set1 complex subunits involved in H2B ubiquitylation-dependent H3K4 methylation. *Nucleic Acids Res* 2018;**46**:11129−43.
20. Talbert PB, Henikoff S. Histone variants on the move: substrates for chromatin dynamics. *Nat Rev Mol Cell Biol* 2017;**18**:115−26.
21. Brand DD, Latham KA, Rosloniec EF. Collagen-induced arthritis. *Nat Protoc* 2007;**2**:1269−75.
22. Tang S, Yao L, Ruan J, Kang J, Cao Y, Nie X, et al. Single-cell atlas of human infrapatellar fat pad and synovium implicates APOE signaling in osteoarthritis pathology. *Sci Transl Med* 2024;**16**: eadf4590.
23. Zhang H, Lin C, Zeng C, Wang Z, Wang H, Lu J, et al. Synovial macrophage M1 polarisation exacerbates experimental osteoarthritis partially through R-spondin-2. *Ann Rheum Dis* 2018;**77**:1524−34.
24. Kapoor M, Martel-Pelletier J, Lajeunesse D, Pelletier JP, Fahmi H. Role of proinflammatory cytokines in the pathophysiology of osteoarthritis. *Nat Rev Rheumatol* 2011;**7**:33−42.
25. Feldmann M, Maini RN. Anti-TNF alpha therapy of rheumatoid arthritis: what have we learned?. *Annu Rev Immunol* 2001;**19**:163−96.
26. Marsh DJ, Ma Y, Dickson KA. Histone monoubiquitination in chromatin remodelling: focus on the histone h2b interactome and cancer. *Cancers (Basel)* 2020;**20**:1−24.
27. Garrido Castro P, Van Roon EHJ, Pinhanços SS, Trentin L, Schneider P, Kerstjens M, et al. The HDAC inhibitor panobinostat (LBH589) exerts *in vivo* anti-leukaemic activity against MLL-rearranged acute lymphoblastic leukaemia and involves the RNF20/RNF40/WAC-H2B ubiquitination axis. *Leukemia* 2018;**32**: 323−31.
28. Lee JS, Shukla A, Schneider J, Swanson SK, Washburn MP, Florens L, et al. Histone crosstalk between H2B monoubiquitination and H3 methylation mediated by COMPASS. *Cell* 2007;**131**:1084−96.
29. Sun ZW, Allis CD. Ubiquitination of histone H2B regulates H3 methylation and gene silencing in yeast. *Nature* 2002;**418**:104−8.
30. Xue H, Yao T, Cao M, Zhu G, Li Y, Yuan G, et al. Structural basis of nucleosome recognition and modification by MLL methyltransferases. *Nature* 2019;**573**:445−9.
31. Hong SH, Cho YW, Yu LR, Yu H, Veenstra TD, Ge K. Identification of JmjC domain-containing UTX and JMJD3 as histone H3 lysine 27 demethylases. *Proc Natl Acad Sci U S A* 2007;**104**:18439−44.
32. Cao R, Wang L, Wang H, Xia L, Erdjument-Bromage H, Tempst P, et al. Role of histone H3 lysine 27 methylation in Polycomb-group silencing. *Science* 2002;**298**:1039−43.
33. Macrae TA, Fothergill-Robinson J, Ramalho-Santos M. Regulation, functions and transmission of bivalent chromatin during mammalian development. *Nat Rev Mol Cell Biol* 2023;**24**:6−26.
34. David-Morrison G, Xu Z, Rui YN, Charng WL, Jaiswal M, Yamamoto S, et al. WAC regulates mTOR activity by acting as an adaptor for the TTT and pontin/reptin complexes. *Dev Cell* 2016;**36**: 139−51.
35. Adamik J, Pulugulla SH, Zhang P, Sun Q, Lontos K, Macar DA, et al. EZH2 supports osteoclast differentiation and bone resorption *via* epigenetic and cytoplasmic targets. *J Bone Miner Res* 2020;**35**: 181−95.
36. Kato H, Asamitsu K, Sun W, Kitajima S, Yoshizawa-Sugata N, Okamoto T, et al. Cancer-derived UTX TPR mutations G137V and D336G impair interaction with MLL3/4 complexes and affect UTX subcellular localization. *Oncogene* 2020;**39**:3322−35.
37. Kamikawa YF, Donohoe ME. The localization of histone H3K27me3 demethylase Jmjd3 is dynamically regulated. *Epigenetics* 2014;**9**: 834−41.
38. Kruidenier L, Chung CW, Cheng Z, Liddle J, Che K, Joberty G, et al. A selective jumonji H3K27 demethylase inhibitor modulates the proinflammatory macrophage response. *Nature* 2012;**488**:404−8.
39. McInnes IB, Schett G. The pathogenesis of rheumatoid arthritis. *N Engl J Med* 2011;**365**:2205−19.

40. Yang X, Zhao Y, Wei Q, Zhu X, Wang L, Zhang W, et al. GRK2 inhibits Flt-1^{+} macrophage infiltration and its proangiogenic properties in rheumatoid arthritis. *Acta Pharm Sin B* 2024;**14**:241−55.
41. Li S, Lin J, Wang C, Liu J, Wang Y, Chen Y, et al. Synergistic metabolic modulation of fibroblast-like synoviocytes *via* targeted dual prodrug nanoparticles to mitigate rheumatoid arthritis. *Acta Pharm Sin B* 2025;**15**:542−56.
42. Martel-Pelletier J, Barr AJ, Cicuttini FM, Conaghan PG, Cooper C, Goldring MB, et al. Osteoarthritis. *Nat Rev Dis Primers* 2016;**2**:16072.
43. Achudhan D, Liu SC, Lin YY, Huang CC, Tsai CH, Ko CY, et al. Antcin K inhibits TNF-α, IL-1β and IL-8 expression in synovial fibroblasts and ameliorates cartilage degradation: implications for the treatment of rheumatoid arthritis. *Front Immunol* 2021;**12**:790925.
44. Liao CR, Wang SN, Zhu SY, Wang YQ, Li ZZ, Liu ZY, et al. Advanced oxidation protein products increase TNF-α and IL-1β expression in chondrocytes *via* NADPH oxidase 4 and accelerate cartilage degeneration in osteoarthritis progression. *Redox Biol* 2020;**28**:101306.
45. Wojtowicz-Praga S. Clinical potential of matrix metalloprotease inhibitors. *Drugs R D* 1999;**1**:117−29.
46. Krzeski P, Buckland-Wright C, Bálint G, Cline GA, Stoner K, Lyon R, et al. Development of musculoskeletal toxicity without clear benefit after administration of PG-116800, a matrix metalloproteinase inhibitor, to patients with knee osteoarthritis: a randomized, 12-month, double-blind, placebo-controlled study. *Arthritis Res Ther* 2007;**9**:R109.
47. Huang YF, Wang G, Ding L, Bai ZR, Leng Y, Tian JW, et al. Lactate-upregulated NADPH-dependent NOX4 expression *via* HCAR1/PI3K pathway contributes to ROS-induced osteoarthritis chondrocyte damage. *Redox Biol* 2023;**67**:102867.
48. Hu J, Zhai C, Hu J, Li Z, Fei H, Wang Z, et al. MiR-23a inhibited IL-17-mediated proinflammatory mediators expression *via* targeting IKKα in articular chondrocytes. *Int Immunopharmacol* 2017;**43**:1−6.
49. Marsolier J, Prompsy P, Durand A, Lyne AM, Landragin C, Trouchet A, et al. H3K27me3 conditions chemotolerance in triple-negative breast cancer. *Nat Genet* 2022;**54**:459−68.
50. Dai J, Yu D, Wang Y, Chen Y, Sun H, Zhang X, et al. Kdm6b regulates cartilage development and homeostasis through anabolic metabolism. *Ann Rheum Dis* 2017;**76**:1291−9.
51. Cribbs AP, Terlecki-Zaniewicz S, Philpott M, Baardman J, Ahern D, Lindow M, et al. Histone H3K27me3 demethylases regulate human Th17 cell development and effector functions by impacting on metabolism. *Proc Natl Acad Sci U S A* 2020;**117**:6056−66.
52. Jun Z, Xinmeng J, Yue L, Zhi W, Yan Z, Tieyi Y, et al. Jumonji domain containing-3 (JMJD3) inhibition attenuates IL-1β-induced chondrocytes damage *in vitro* and protects osteoarthritis cartilage *in vivo*. *Inflamm Res* 2020;**69**:657−66.
53. Pinzi L, Rastelli G. Molecular docking: shifting paradigms in drug discovery. *Int J Mol Sci* 2019;**20**:4331.
54. Wang JN, Wang F, Ke J, Li Z, Xu CH, Yang Q, et al. Inhibition of METTL3 attenuates renal injury and inflammation by alleviating TAB3 m6A modifications *via* IGF2BP2-dependent mechanisms. *Sci Transl Med* 2022;**14**:eabk2709.
55. Reid IR, Bolland MJ, Grey A. Effects of vitamin D supplements on bone mineral density: a systematic review and meta-analysis. *Lancet* 2014;**383**:146−55.
56. Wesseling-Perry K, Pereira RC, Sahney S, Gales B, Wang HJ, Elashoff R, et al. Calcitriol and doxercalciferol are equivalent in controlling bone turnover, suppressing parathyroid hormone, and increasing fibroblast growth factor-23 in secondary hyperparathyroidism. *Kidney Int* 2011;**79**:112−9.
57. Moe SM, Saifullah A, LaClair RE, Usman SA, Yu Z. A randomized trial of cholecalciferol *versus* doxercalciferol for lowering parathyroid hormone in chronic kidney disease. *Clin J Am Soc Nephrol* 2010;**5**:299−306.
58. Gao XR, Chen YS, Deng W. The effect of vitamin D supplementation on knee osteoarthritis: a meta-analysis of randomized controlled trials. *Int J Surg* 2017;**46**:14−20.
59. Chen X, Gong W, Shao X, Shi T, Zhang L, Dong J, et al. METTL3-mediated m6A modification of ATG7 regulates autophagy−GATA4 axis to promote cellular senescence and osteoarthritis progression. *Ann Rheum Dis* 2022;**81**:87−99.
60. Lin NY, Beyer C, Giessl A, Kireva T, Scholtysek C, Uderhardt S, et al. Autophagy regulates TNFα-mediated joint destruction in experimental arthritis. *Ann Rheum Dis* 2013;**72**:761−8.